ELSEVIER

The Science of the Total Environment 167 (1995) 87–101

the Science of the Total Environment
An International Journal for Scientific Research into the Environment and its Relationship with Man

Nature and decay effects of urban soiling on granitic building stones

N. Schiavon*[a], G. Chiavari[b], G. Schiavon[b], D. Fabbri[c]

[a]*Department of Earth Sciences, Cambridge University, Cambridge, UK*
[b]*Dipartimento di Chimica 'Ciamician', Bologna University, Bologna, Italy*
[c]*Laboratorio di Chimica Ambientale, Ravenna, Bologna University, Bologna, Italy*

Abstract

A detailed microscopical and chemical examination by SEM + EDAX, XRD and Py/GC-MS of black patinas coating the surfaces of urban granitic monuments in Aberdeen and Dublin has revealed a variety of decay features together with a complex chemical composition. Beside sulphate-rich thick patinas composed of a framework of gypsum crystals in which both particulate and gaseous inorganic/organic pollutants are deposited and which are similar to gypsum crusts developing under polluted atmospheric conditions on calcite-bearing stones, thinner, gypsum-free, black surface layers made up of particulate matter embedded in a fine-grained, iron-rich matrix are commonly found. These soiling layers show, relative to the substrate, higher % of P, Ca, S, and Cl. The occurrence of a patina's type against the other is probably controlled by the availability of local SO_2 sources. Physical and chemical decay effects on the granitic substrate are more severe when gypsum is present but dissolution and micro fracturing episodes are also observed in iron-rich patinas. The chemical inorganic/organic composition of these surficial layers suggests that pollution induced soiling processes are the main factors responsible for their build-up on building facades. On the other hand, microscopic and preliminary chemical evidence does not exclude biological activity as an important agent in the development of iron-rich thin black layers.

Keywords: Granitic buildings; Urban soiling; Black patinas; Gypsum patinas; Iron-rich patinas; Granite buildings; Gypsum/silicate replacement; Black patinas; Analytical pyrolysis

1. Introduction

The surface soiling of stone monuments and works of art exposed to polluted urban atmospheres has become the object of intense research amongst conservation scientists in recent years. The problem that these surficial patinas cause to the preservation of our artistic cultural heritage is not only an aesthetic one; weathering and decay processes acting on the stone substrate underneath are a common feature. This is true not only in 'soft' highly porous stones such as limestones and calcite-cemented sandstones but also in 'hard' low porous stones such as granite [1–5]. Granite is an igneous rock with a multimin-

* Corresponding author.

SSDI 0048-9697(95)04572-5

eralogical (although primarily silicate) composition. Preliminary results on granite samples from urban localities in the Iberian Peninsula [5] have revealed how compositionally complex the soiling layers might be and how their decay effects on the substrate may vary according to parameters such as the stone mineralogy and the nature of air pollution surrounding the monuments under study.

An in-depth understanding of the weathering processes operating at the stone-patina interface, of decay products composition and of their relationship with air pollution is essential in the correct choice of cleaning procedures and conservation policies to be applied to each case study. It can also prove useful in assessing the extent to which low porosity granitic building stones (as it is the case with more porous lithologies) may act as sinks for atmospheric airborne pollutants.

In this paper, we combine different analytical techniques (SEM + EDAX, XRD, Pyrolysis /GC-MS) to characterise the inorganic-organic composition of and the decay features associated with black patinas coating the surfaces of granitic building stone in two northern European cities: Aberdeen, UK and Dublin, Ireland.

2. Sampling sites

Samples of surficial soiled layers (together with fragments of the underlying granitic substrate) were collected from the following buildings:

2.1. Regent's House, Trinity College, Dublin, Ireland

Black weathering crusts were collected from chimney stacks on the roof of the Regent's House (1752–1759), Trinity College. Most of the granite used in the College's historic buildings comes from a quarry at Golden Hill, some 30 km SW of Dublin; this granite (Leinster Granite) is part of a granitic alkaline complex intruded during the Caledonian orogeny in SE Ireland. The main minerals present are quartz, microcline and orthoclase (in roughly equal proportions), highly weathered plagioclase, muscovite and chloritised biotite; accessory minerals include zircon ($ZrSiO_4$), rutile (TiO_2), monazite [$(Ce,Th)PO_4$] and Mn-rich garnet $(Mn,Fe)_3Al_2Si_3O_{12}$.

The College is situated in a city centre area just south of the old estuary of the river Liffey; the area is characterised by medium–high levels of air pollution from vehicular traffic. High-sulphur coal has been extensively used as a fossil fuel for industrial and domestic heating purposes until the recent introduction in Ireland of government clean air regulations. SO_2 annual pollution levels in the Dublin city area for the period 1979–1991 averaged 38 $\mu m/m^3$ (with a marked decrease from 44 $\mu m/m^3$ in 1979 to 21 $\mu m/m^3$ in 1991). The climate is that of a sheltered western seaboard urban conurbation; a local pollution-related greenhouse effect is responsible for the creation of an urban heat island which, in turn, results in slightly elevated air temperatures and increased cloud cover.

2.2. York Street Nursery School, Footdee, Aberdeen, UK

This school is approximately 100 years old and is situated close to the Aberdeen tidal harbour less than 100 m from the city's North Sea shore; the building is included in a research programme into stone-cleaning of granite which is being carried out by the Robert Gordon Institute of Technology, Faculty of Design, Aberdeen. No information is available on the precise source of the granite although its local origin is almost certain, due to the large number of granite quarries known to have been used for building purposes in the Aberdeen area in the past 200 years. Flakes of soiled granite attached to underlying blistered and spalling granite were collected from vertical walls between 1.5 and 3 m in height. Mineralogically, the granite contains quartz as the most abundant mineral with common plagioclase, K-feldspar and weathered biotite; non-silicate accessory minerals (usually present as small inclusions) include apatite (Ca_5PO_5), rutile, ilmenite ($FeTiO_4$), sphene ($CaTiSiO_4$) and iron oxides (magnetite?).

Meteorological data (kindly supplied by the Aberdeen Meteorological Office) show an average annual precipitation for the last 30-year pe-

riod of 789 mm/annum. SO_2 levels in the city, recorded at a monitoring station situated approximately 1 mile from the York School sampling site, show a mean % for the period 1984–1993 of 29.3 $\mu g/m^3$.

3. Experimental

Both rough specimen surfaces and polished thin-sections of the granitic chips spanning the contact stone-patinas were microscopically examined. The thin sections were hand polished down to a thickness of 60–70 μm (much thicker than the standard 30 μm used for routine petrographic studies). This technique proved useful in avoiding loss of material due to differences in hardness between the original granitic stone and the decay patinas present on its surface. After sputter coating with a thin carbon layer to avoid charging effects, the sections were examined in a Jeol 820L SEM (with back-scattered detector) interfaced with a Link 860 EDAX system using the ZAF4/FLS quantitative analysis software. The back-scattered mode is particularly useful in the study of materials with a complex composition such as the black patinas because of the correlation between levels of brightness in the BSEM image and the elemental composition of the area under investigation.

XRD was performed on patina powders scratched from the surface of the samples using a Philips PW Vertical Goniometer. Operating conditions: Cu Kα radiation (1.548 Å) with Ni filter; 40 Kv, 20 Ma; time constant, 1–400 c.p.s.; divergent slit, 1; receiving slit, 0.5.

Pyrolysis-gas chromatography/mass spectrometry (Py-GC/MS) was performed with an integrated system consisting of a heated filament pyrolyser (CDS 1000 Pyroprobe) fitted with a platinum coil probe and quartz tube sample holder, a Varian Saturn II capillary gas chromatograph/ion trap mass spectrometer equipped with a J&W DB5 column (30 m × 0.32 mm i.d., 0.25 μm film thickness). The Py-GC/MS instrument was operated under the following conditions: pyrolysis at 700°C for 20 s, Py-GC interface at 200°C; GC injector at 250°C, gas chromatography from 50°C (held for 2 min) to 280°C at 5°C min^{-1}. The split injection mode was used (split ratio 1:180). Mass spectra (1 scan s^{-1}) were recorded under electron impact at 70 eV using ion trap detector software Release 4.0, from m/z 40 to 450. Weighed samples (less than 10 mg of patina) were pyrolysed. Repeated test with blanks showed a limited build-up of instrumental contamination (mainly silicones) whose peaks were stripped from the final TIC charts.

4. Results and discussion

4.1. SEM + EDAX observations

Dublin

A gypsum-rich patina up to 0.5 cm thick can be seen coating the surface of the building stone. The weathering crust is made up of a dense network of platy and acicular gypsum crystals with, macroscopically, a dendritic, high porosity texture (Fig. 1). Physical fragmentation of the granite micro fabric is the most obvious decay feature; mineral fragments (plagioclase, K-feldspar, biotite flakes, quartz), clearly derived from the stone substrate, can be seen embedded deep inside the black patina (Fig. 1); besides the stone contribution, other particulate material (of likely

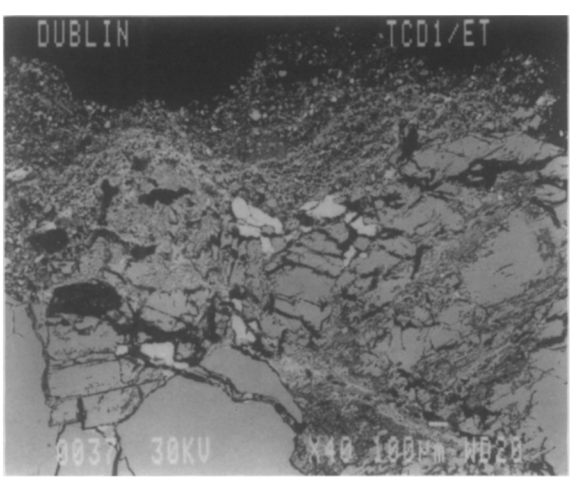

Fig. 1. Dublin. Gypsum-rich patina on granite. Note almost total breakdown of granite's fabric into mineral fragments which are eventually incorporated into the weathering crust, together with spherical micron-size particles of anthropogenic origin.

atmospheric origin) include Fe-rich fragments, carbonaceous cenospheres with a mainly Ca-S composition and spherical particles (10 μm in diameter) with an aluminosilicate and/or Ca-Fe composition.

Besides the readily apparent mechanical disruption of the stone outermost surface, there is also evidence of chemical interactions between the weathering solutions responsible for the precipitation of gypsum and the granite minerals: microscopic evidence suggesting replacement of primary silicate minerals by Ca-sulphate dehydrate salts is quite common (Fig. 2). In many cases, the outline of the primary silicate is still preserved after total gypsum replacement (Fig. 3) while in others the process is present at an intermediate stage (Fig. 2). This situation is reflected in the elemental composition of the area subjected to chemical replacement where relative differences in the intensities of sulphate-related (Ca, S) vs. silicate-related (Si, Al, Na, K) peaks can be visually correlated by EDAX analysis with degree of replacement. Although episodes of chemical dissolution at the contact patina-stone are commonest when alkali-feldspars and plagioclases constitute the mineral substrate, quartz dissolution also seems to occur (Fig. 4).

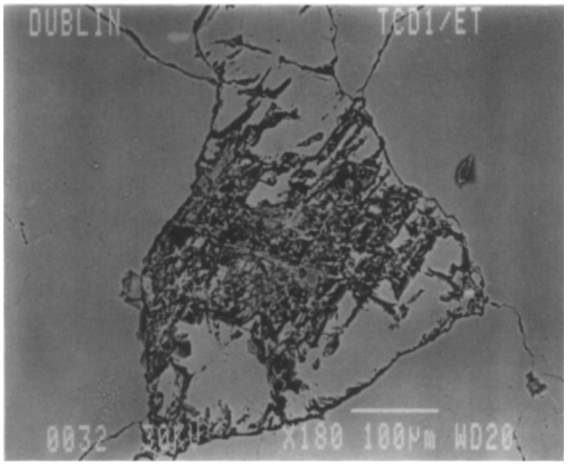

Fig. 2. Dublin. Plagioclase inclusion within quartz 5–10 mm away from the stone-patina interface. Plagioclase is undergoing partial replacement by gypsum. Microfractures in quartz seem to have acted as pathways for gypsum crystallising solutions inside the granite.

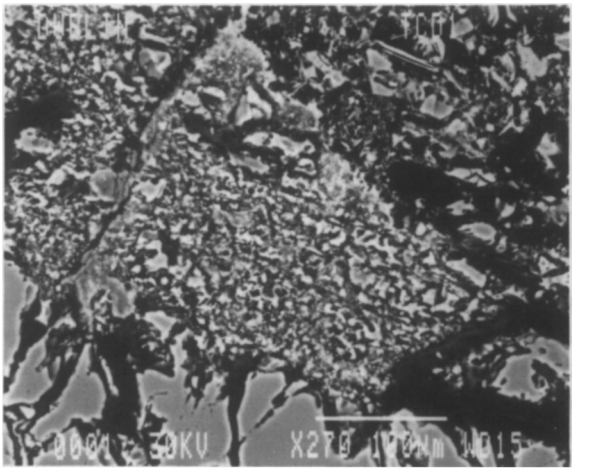

Fig. 3. Dublin. Contact between gypsum patina and granite showing a feldspar mineral totally replaced by gypsum. Note how the original outline of the silicate mineral can still be seen.

Examination of the rough surfaces of samples in secondary mode, reveals the fairly discontinuous character of the gypsum-rich patinas and the tendency of gypsum crystals to form cluster aggregates. A very high number of smooth, spherical, micron-size particles with an aluminosilicate composition are evident on the granitic substrate (Fig. 5). No evidence of biological material colonising the surface of the granite was found.

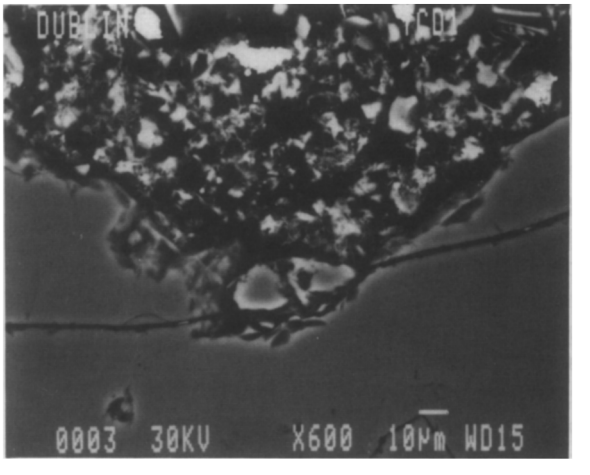

Fig. 4. Dublin. Contact between gypsum patina and granite showing quartz dissolution.

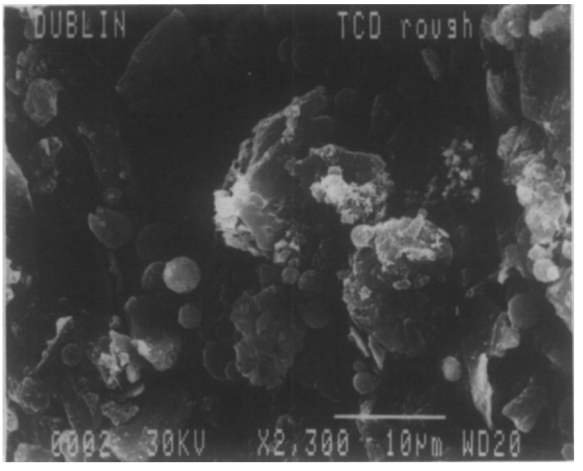

Fig. 5. Dublin. Granite's surface coated with gypsum crust. Note high abundance of smooth, spherical, micron-size particles with an Al-Si composition, typical by-products of coal combustion processes.

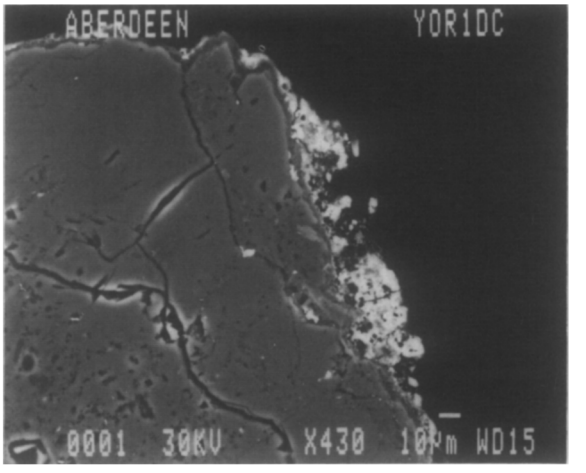

Fig. 6. Aberdeen. Thin, discontinuous, iron-rich (brighter under back-scattered SEM investigation) patinas on granite. Note high porosity and faint laminated structure.

X-Ray powder diffraction (XRD) confirms gypsum as the only 'alien' crystalline component in the crusts besides chart peaks belonging to mineral fragment derived from the stone itself (i.e. quartz, feldspars, micas).

Aberdeen

Thin patinas, ranging in thickness between 0 and 20 μm, are present as discontinuous coatings on the outer granite surface. When well developed, patinas display a typical spongy, high porosity texture showing, at times, pseudo lamination micro fabric (Fig. 6). They are often associated with decay affecting the granitic substrate underneath: a number of fractures and micro cracks running parallel to the stone surface up to a depth of several mm and leading to the disintegration and eventual detachment of granite scales are lined with desegregated debris, iron oxides and micron-size spherical particles of likely anthropogenic origin; evidence of dissolution and fracturing is common not only on plagioclase's and feldspar's but also on 'geochemically' stable quartz's surfaces. The surface desegregation may lead to the formation of surface patinas totally made up of comminuted stone fragments (Fig. 7).

Despite the granite multimineralogical composition, the patinas elemental composition does not differ substantially from one place to the other; EDAX analysis shows that, relative to the unweathered mineral substrate, the patinas show higher concentrations of Fe, P, Ca, S, and Cl. Areas showing an Al only composition have been interpreted as fine-grained gibbsite ($Al[OH]_3$), a common decay product of natural weathering of silicate minerals. 'Alien' components of the patinas whose origin may be connected with air pollu-

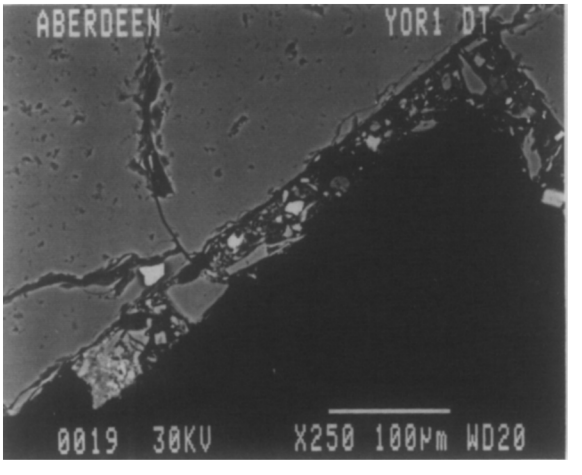

Fig. 7. Aberdeen. Patina on quartz mineral substrate composed of loose debris including mineral fragments from the granitic stone, soil dust and particulate pollutants.

tion include $BaSO_4$ (baryte) seen precipitating within micro cracks in quartz and between biotite cleavage planes and $PbSO_4$ (cerussite) again precipitating along mineral fractures; authigenic crystals with a KCl composition (probably silvite salts), which are not present as primary minerals in granitic rocks, can occasionally be seen, especially on quartz surfaces. Spherical and pseudo-spherical micron-size particles are found embedded within the patina's matrix, inside fractures a few mm deep inside the stone and also trapped within mica's cleavage planes (Fig. 8): their size, morphology, iron-rich and/or aluminosilicate elemental composition together with their smooth micro texture suggest an origin from coal combustion processes. Their abundance here, however, is rather low compared to that reported in gypsum-rich surficial patinas.

Examination of the outer rough surface of the granitic chips, before thin-section preparation, while confirming the BSEM results in showing the granite surface coated either with loose desegregated mineral fragments and/or with an amorphous, smooth iron-rich deposit (Fig. 9), also shows the presence of biocolonisation in the form of biogenic filaments (collapsing under electron beam exposure) forming bridges between mineral grains. Authigenic Ca-phosphate crystals with a well-developed mineral habit (apatite?) are occasionally found within the surface patina.

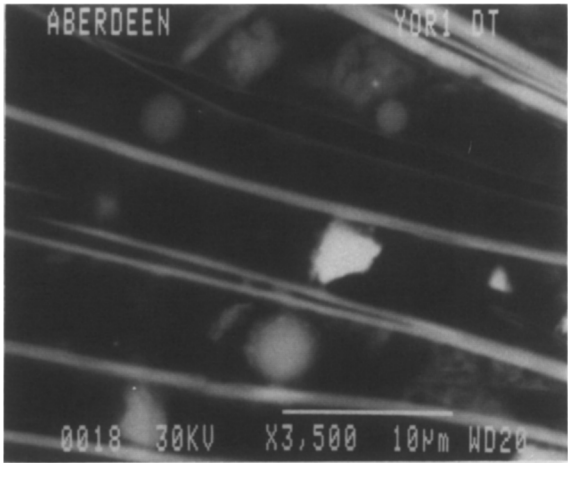

Fig. 8. Aberdeen. Spherical particles of about 10 μm in diameter with an Al-Si and/or a Fe composition (typical by-products of fossil fuel combustion processes) trapped between cleavage planes in biotite.

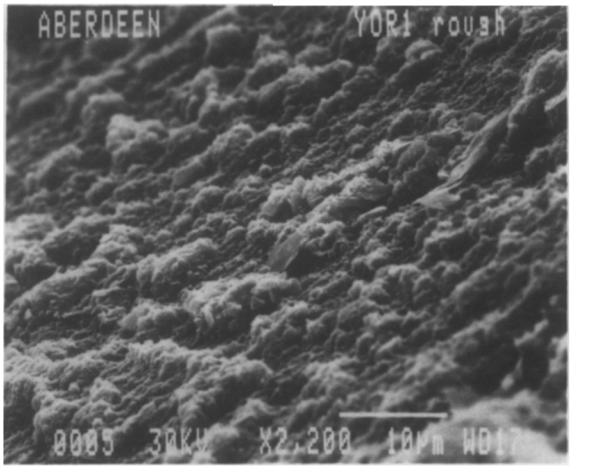

Fig. 9. Aberdeen. Surface of granite coated with micron-size iron-rich precipitates.

X-Ray powder diffraction (XRD) identified only crystalline compounds known to be granite's primary mineral constituents. This suggests that the iron-rich matrix is predominantly made up of amorphous iron oxides–hydroxides.

Gypsum vs. iron-rich patinas

As with previous examples of black patinas on granite [5], soiled layers of different composition and responsible, in turn, for distinct decay features are seen coating the surface of the building stone. The single most important discriminating factor between the different patinas is the presence (or absence) of a sulphate-rich component (i.e. gypsum); well defined thick gypsum crusts are present here in the Trinity College samples.

The presence and abundance of gypsum may be controlled by the following factors: (1) supply of the Ca^{++} and SO_4^{--} ions necessary for gypsum growth; (2) location of the sample in the monument with respect to rain wash-out episodes leading to secondary gypsum dissolution.

(1) An atmospheric origin for the sulphate anions is very likely, taking into account the very low amount of S-rich minerals in granitic rocks and the fact that mortars used in the buildings examined here do not contain any sulphate. Fur-

thermore, the Trinity College patinas were collected on chimney stacks known to have discharged (at least for the last two centuries) high sulphur-coal smoke into the Dublin atmosphere; the abundance of aluminosilicate micron-size spherical particles in the same patinas (a typical by-product of coal combustion processes; Fig. 5) confirms the relative importance of a pollution source so close to the sampling site.

The origin for the Ca^{++} cations is more controversial. Calcitic soil dust, or Ca-rich airborne particulate pollutants including carbonaceous cenospheres from domestic and industrial oil burning [4] have been claimed as possible Ca^{++} sources. In view of the relatively low abundance of Ca-rich particles embedded within the patinas, however, it is unlikely that these sources can volumetrically account for the observed widespread Ca-sulphate precipitation: gypsum crusts are particularly well-developed near mortar joints and/or below limestone decorative architectural features such as window sills and we then suggest, following Cooper et al. [1], that the main gypsum precipitating mechanism is the reaction of Ca-rich lime mortar (and/or limestone leached Ca^{++} ions) with atmospheric SO_2. Airborne particulate pollutants may then accelerate the S-related decay process by acting as catalysts in the oxidation of sulphur dioxide.

(2) The location of the stone substrate with respect to rain wash-out episodes has been shown to play an important role in the build up of sulphate crusts on carbonate stone [6]. This discriminating factor should act independently from the mineralogical composition of the stone and be affected only by the amount of driving rain on the stone surface able to leach away already precipitated salts. One may then argue that gypsum-free thin dark patinas on granite might represent nothing more than areas where gypsum precipitation did take place but was followed by leaching episodes; however, their presence in areas where there is little or no wash-out [5] and their quite distinctive texture and composition does not favour this hypothesis. It is more likely that the local availability of SO_2 sources is more important in controlling gypsum precipitation.

When a sulphate component is not present (or is present in very low %), soiling processes on granite tend to produce thinner iron-rich patinas such as the ones coating the York School's building walls in Aberdeen. The inorganic chemical composition of these patinas appears to remain remarkably constant in monuments and buildings exposed to different environmental and climatic conditions [2,5] and consists essentially of mineral fragments detached from the stone, soil dust particles and particulate matter of likely anthropogenic origin embedded in an amorphous iron-rich matrix with P and Cl as important accessory elements. The iron in the patinas is likely to come from leaching of iron-bearing minerals in the granite (such as biotite and iron oxides, [2,5]). P (mostly present in the patinas as amorphous phosphates and, less commonly, as individual apatite crystals) may also have been released from P-bearing minerals in the granite such as apatite, quite common in the Aberdeen granite and absent in Dublin examples; whereas a sea-spray source for Cl, present as KCl (and probably also as trace amounts of NaCl) salts, is quite likely considering the absence of chlorides in granitic rocks and the relative closeness of the Aberdeen site to the sea shore.

It has been assumed, taking into account their urban location and their chemical composition, that these iron-rich thin soiling layers are the result of dry-wet deposition of airborne particulate and gaseous pollutants on buildings [2]; our observations (see also the chemical section below) confirm the presence in the Aberdeen patinas of constituents (in particular airborne particulate matter from coal combustion and oil combustion, lead and barium precipitates) clearly derived from anthropogenic emission sources: it is important to note, however, how these gypsum-free soiling layers resemble quite closely, in their iron-rich composition, particulate morphology of the iron deposits (Fig. 9) and in their micro fabric (pseudo lamination, see Fig. 1 in [7]), desert varnish deposits for which a biologically mediated mechanism of growth is widely assumed [8]; the ability of bacteria, fungi and lichens to concentrate and precipitate Fe and P compounds is indeed well known [7–9] as well as the role that microbially produced organic acids and complexing com-

pounds may have in increasing the solubility of silicate and quartz minerals [9,10]. Redox reactions involving iron have been reported to lead to increased solubility of quartz also in laboratory experiments [11], probably because oxidation causes breakdown of an ultra thin ferrous iron/silica complex formed on the quartz surface with accompanying liberation of silica. Swift alternations, on a microscopic scale, of redox conditions would be expected within surface patinas on building facades especially if iron-reducing and iron-oxidising bacterial activity is present [9].

Gypsum / silicate replacement

Contrary to previous research which suggested sulphation induced decay on non-calcite-bearing low porosity stones (such as granites) as a predominantly physical decay process promoting the creation of fractures through salt crystallisation energies, petrographical evidence is presented here suggesting also chemical reactions between granite mineralogy and weathering solutions precipitating gypsum; feldspar minerals partially or totally replaced by sulphate crystalline salts while still retaining their primary mineral outline and texture (Figs. 1,3); selective replacement of plagioclase inclusions within quartz crystals where no displacive movement is present nor possible due to the physical restraint of the surrounding quartz (Fig. 2); and weathering front prograding inside mineral surfaces away from pre-existing fractures and weakness lines (Fig. 4). All of these observations suggest a chemically active decay. In many cases, the replacement reactions leading to the transformation of primary silicate minerals into secondary sulphate salts appear to be the consequence of a pseudomorphism process without a substantial change in shape and volume of the crystals (Figs. 1,3). Pseudomorphism of gypsum after calcite has been reported as the process responsible for the development of clear gypsum layers at the contact between badly decayed marble and sulphated crusts [12]; in this study, four steps are envisaged in the decay process: (a) marble thermal fracturing; (b) precipitation of gypsum rims lining cracks and cleavages; (c) dissolution of calcite by sulphuric acid with formation of a hollow gypsum boxwork and (d) precipitation of gypsum within all the remaining voids. In the case of the granite samples examined here, microscopic evidence is compatible with the presence of steps (a) and (b) but not of steps (c) and (d): a simple dissolution reaction between sulphuric acid and the silicate minerals (as it is the case with carbonate minerals) is not likely due to the much lower solubility of silicates and quartz compared with calcite. Indeed silica is not readily attacked by inorganic acids such as H_2SO_4 and normally requires strong alkaline conditions (pH > 9) for its dissolution. A likely mechanism for gypsum replacement of silicate minerals may involve the localisation of silicate dissolution and gypsum precipitation to thin solution films between the silicate and sulphate phases; according to this model, the dissolution of silicates and the precipitation of gypsum should occur simultaneously and original textural features in the primary mineralogy can be preserved after replacement. In order to explain undersaturation of silicates and supersaturation with respect to gypsum at the same time and space, we may recall a model originally proposed by Maliva and Siever [13] for the silicification of calcitic fossils. In their study, the authors believe that the force of crystallisation (defined as the pressure a crystal is able to bear or grow against at a given degree of supersaturation) of silica may result in a local increase in calcite solubility at the contact surface between crystallising mineral and adjacent crystals. Although this model was originally proposed to explain the replacement of calcium carbonate minerals by silica, in principle its validity should not be confined to a silica/carbonate system [13]; the most important factors controlling the replacement mechanism are in fact degree of supersaturation of the gypsum precipitating solutions and relative crystallisation pressures arising from these precipitation episodes. Winkler and Singer [14] have calculated that gypsum energies of crystallisation may produce pressures exceeding 1900 atm (at 50% of supersaturation); these pressures may then be responsible not only for displacive physical decay effects already reported on weathered granitic surfaces [1–5], but also for the chemical replacement observed in this study (particularly when gypsum growth occurs within a spatially

restricted area where no displacive movement is allowed such as inclusions within a rigid framework of a host mineral like quartz; Fig. 2). The replacement is most effective on feldspars, probably because of their higher surface area susceptible to chemical attack (due to the abundance of intracrystalline fractures and microcracks due to their higher chemical reactivity) together with their lower density with respect to quartz; mica's typical platy morphology and perfect basal cleavage does not seem to favour chemical decay but rather the physical detachment of the crystal's layers.

4.2. Analytical pyrolysis

Preliminary results by analytical pyrolysis combined with GC/MS of black soiling from the two sites investigated are presented in Tables 1 and 2 with the corresponding Total Ion Current traces (TIC) in Figs. 10 and 11.

Dublin

The organic compounds identified in black patinas from Trinity College (Table 1 and Fig. 10) can be broadly grouped into the following categories: alkanes, alkenes, aromatic hydrocarbons and derivatives, polyaromatic hydrocarbons (PAH), aldehydes and ketones, N-containing compounds.

Alkanes. We have identified the complete series of homologs ranging from C_{10} to C_{18} with a Carbon Preference Index (CPI) = 0.8 with the most abundant homologs (C_{max}) in the C_{11}–C_{15} range. The CPI is the sum of the odd-carbon-number homologs over a specified range divided by the sum of the even-carbon-number over the same range and has been utilised as a diagnostic tool for estimating the relative importance of biogenic vs. anthropogenic sources of organic pollutants [15]. A CPI value near unity combined with a low C_{max} for n-alkanes suggests an anthropogenic origin from fossil fuel combustion; more specifically, it is characteristic of petroleum residues and vehicular exhaust emissions [15–17].

Alkenes. We have identified the complete series of homologs ranging from C_{10} to C_{18} again with a CPI = 0.8 and a C_{max} in the range C_{10}–C_{14}. These alkenes derive probably from pyrolytic decarboxylation of fatty acids [15]: n-alk-1-enes. Sources contributing n-fatty acids to fine atmospheric aerosols are similar to the emission sources of n-alkanes discussed earlier; they include the combustion of fossil fuels, wood and organic detritus. Alkenes are also obtained in industrial quantities chiefly by the cracking of petroleum.

Aromatic hydrocarbons and derivatives. Anthropogenic pollution sources are responsible for the

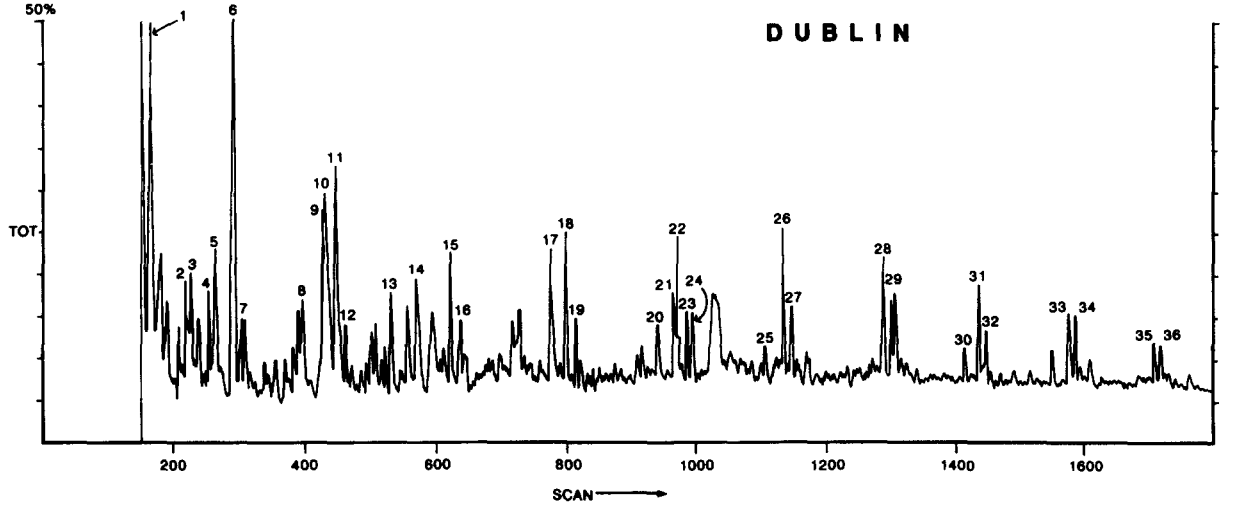

Fig. 10. Py/GC-MS chromatogram of black patinas from Trinity College, Dublin.

Table 1
Proposed identification of the main pyrolysate fragments from Py-GC/MS analysis of black patinas from Trinity College Dublin, Ireland

Peak No.	Scan No.	%[a]	MW	Compounds
1	164	100	92	Toluene
2	228	26	81	2-Methyl-pyrrole
3	239	8	81	3-Methyl-pyrrole
4	254	17	106	Ethylbenzene
5	265	23	106	*m* + *p*-Xylene
6	291	121	104	Styrene
7	306	10	106	*o*-Xylene
8	391	8	106	Benzaldehyde
9	430	38	—	Unknown
10	432	43	94	Phenol
11	449	39	140	1-Decene
12	464	10	142	n-Decane
13	533	17	116	Indene
14	571	21	120	Acetophenone
15	623	24	154	1-Undecene
16	639	18	156	n-Undecane
17	777	24	128	Naphthalene
18	801	27	168	1-Dodecene
19	816	12	170	n-Dodecane
20	942	14	132	2,3 Dihydro-1-H-indene-1-one
21	967	19	142	1-Methyl-naphthalene
22	972	30	182	1-Tridecene
23	986	16	184	n-Tridecane
24	995	12	142	2-Methyl-naphthalene
25	1109	7	154	Biphenyl
26	1135	30	196	1-Tetradecene
27	1149	16	198	n-Tetradecane
28	1290	22	210	1-Pentadecene
29	1303	14	212	n-Pentadecane
30	1416	6	166	Fluorene
31	1438	17	224	1-Hexadecene
32	1449	10	226	n-Hexadecane
33	1578	13	238	1-Heptadecene
34	1588	12	240	n-Heptadecane
35	1712	7	252	1-Octadecene
36	1720	7	254	n-Octadecane

[a]% are calculated relative to the toluene peak = 100%.

presence of these compounds in built-up urban areas. Styrene (6; the strongest peak in the TIC from Trinity College), toluene (1), ethylbenzene (4), *o*-, *m*- and *p*-xylenes (5,7) are light alkyl aromatic compounds which may derive from pyrolysis or flash vaporisation of bituminous coal or from pyrolysis of synthetic or natural polymeric materials. They are also typical by-products from industrial refining of petroleum. Polystyrene is between the polymers used in street paving as an additive to bitumen to improve resistance to ageing and to eliminate the 'aquaplaning' effect by increasing asphalt porosity (which in turn facilitate water draining and leads to a reduction of street noise levels).

Polycyclic aromatic hydrocarbons (PAH). The following PAH were identified: indene (13), naphthalene (17), 1-methylnaphthalene (21), 2-methylnaphthalene (24), biphenyl (25), and fluorene (30). PAH are anthropogenic compounds derived from

Table 2
Proposed identification of the main pyrolysate fragments from Py-GC/MS analysis of black patinas from York Nursery School, Aberdeen, UK

Peak No.	Scan No.	%[a]	MW	Compounds
1	164	100	92	Toluene
2	224	129	—	2-Furaldehyde (MW = 96) + Unknown (MW = 82)
3	255	12	106	Ethylbenzene
4	265	19	106	*m* + *p*-Xylene
5	292	28	104	Styrene
6	308	34	96	2-Methyl-cyclopenten-1-one
7	327	24	98	2-Methyl-cyclopentanone
8	391	26	106	Benzaldehyde
9	432	18	—	Phenol (MW = 98) + Benzonitrile (MW = 103)
10	449	22	140	1-Decane
11	502	55	112	2-Hydroxy-3-methyl-2-cyclopenten-1-one
12	515	41	136	Terpenic derivative
13	527	19	110	2,3-Dimethyl-2-cyclopenten-1-one
14	550	23	126	3,4-Dimethyl-2-hydroxy-2-cyclopenten-1-one
15	572	22	120	Acetophenone
16	622	28	154	1-Undecene
17	640	10	156	n-Undecane
18	663	15	126	3-Ethyl-2-hydroxy-2-cyclopenten-1-one
19	801	42	168	1-Dodecene
20	822	22	170	n-Dodecane
21	943	14	132	2,3-Dihydro-1-H-indene-1-one
22	973	29	182	1-Tridecene
23	987	9	184	n-Tridecane
24	1137	37	196	1-Tetradecene
25	1150	10	198	n-Tetradecane
26	1290	22	210	1-Pentadecene
27	1308	12	212	n-Pentadecane
28	1328	28	182	Dibenzyl (or) 1,2-diphenylethane
29	1440	21	224	1-Hexadecene
30	1580	5	238	1-Heptadecene
31	1589	5	240	n-Heptadecane

[a] % are calculated relative to the toluene peak = 100%.

incomplete combustion of organic matter. They are present in oil but are also emitted from incomplete combustion of gasoline and diesel fuels.

Aldehydes and ketones. These compounds probably derive from photochemically induced oxidation reactions in the atmosphere. Benzaldehyde (8) may form through the photooxidation of toluene, although it has also been reported as a primary pollutant entrapped in black crusts in urban areas [18]; 2,3 dihydro-1-H-indene-1-one (20) through the oxidation of the methylene group of indene. The origin of acetophenone (14) is not clear; however, its presence in urban areas as an airborne organic pollutant is known [19].

N-containing compounds. 2-Methyl pyrrole (2) and 3-methyl pyrrole (3) are the only N-containing compounds present in the pyrolysate. They can be present both in coal tar and bone oil, although they also represent pyrolysis products of proteinic material.

Aberdeen

The organic compounds identified in black patinas from York Nursery School (Table 2 and Fig. 11) can be broadly grouped into the following categories: alkanes, alkenes, aromatic hydrocarbons and derivatives, aldehydes and ketones.

Alkanes. Undecane (17), dodecane (20), tridecane (23), tetradecane (25), pentadecane (27),

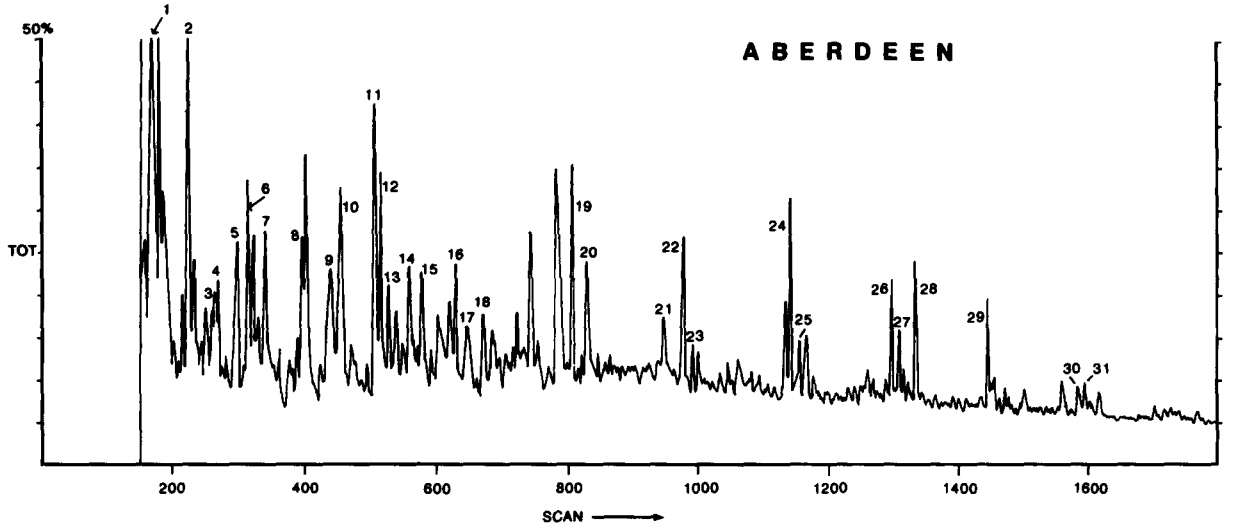

Fig. 11. Py/GC-MS chromatogram of black patinas from York Nursery School, Aberdeen.

heptadecane (31) were identified with a CPI = 2 and C_{12} as the most abundant homolog (C_{max}). Despite the CPI being > 1, which may suggest a plant wax signature (not confirmed however by the presence of high C number homologs typical of a biogenic input), the low carbon number C_{max} again suggests an anthropogenic origin from fossil fuel combustion processes for these alkanes.

Alkenes. The complete series of homologs ranging from C_{10} to C_{17} were identified with a CPI = 1 and with the most abundant homologs (C_{max}) in the range C_{11}–C_{14}. As for the alkenes in Table 1, they probably form through decarboxylation of fatty acids and are dispersed in the atmosphere via the combustion of fossil fuels, organic detritus and wood.

Aromatic hydrocarbons and derivatives. The styrene peak (5) in this pyrogram is considerably lower compared to the same one in the pyrogram of Table 1 with a % (relative to the toluene peak) in Aberdeen patinas of only 28% compared to 121% in Dublin crusts. The toluene peak (1), instead, is still very well developed, despite being 'disturbed' by three unidentified peaks nearby. Ethylbenzene (3) and phenol (9) are also present whereas in Aberdeen patinas we have not found indene. As is the case with the Dublin samples, all of these aromatic hydrocarbons can be attributed to anthropogenic pollution sources. In the TIC from Aberdeen we also found dibenzyl or 1,2-diphenyl ethane (28) with an abundance (relative to the toluene peak = 100%) of 28%. Although it could represent one of the pyrolytic products of the amino acid phenylalanine [20], its identification in the solvent extract of black crusts from the cathedral of Seville [18], suggests that this compound may be commonly present as such in polluted urban atmospheres and does not necessarily derive from pyrolytic degradation.

Aldehydes and ketones. 2-Furaldehyde or furfural (2) is the highest peak in the Aberdeen TIC; it may form as the decomposition product of polysaccharides present in plant cell walls and it has been found in analytical pyrolysis of lichen thalli [21]. Besides compounds present also in Irish samples such as benzaldehyde (8), acetophenone (15) and 2,3 dihydro-1-H-indene-1-one (21) and for which the same sources can be hypothesised, we have found an interesting series of ketonic derivatives of cyclopentene, i.e. 2-methyl cyclopenten-1-one (6), 2-methyl cyclopentanone (7), 2-hydroxy-3-methyl-2-cyclopenten-1-one (11), 2,3-dimethyl-2-cyclopenten-1-one (13), 3,4-dimethyl-2-hydroxy-2-cyclopenten-1-one (14) and 3-ethyl-2-hydroxy-2-cyclopenten-1-one (18); all of these compounds may derive from pyrolysis of

cellulose and so constitute a marker of the presence in the Aberdeen patinas of this polysaccharide.

From the chemical data it can be concluded that in both monuments, the organic fraction of the black patinas is mainly composed of compounds that are characteristic of anthropogenic pollution sources from the burning of petroleum derivatives and/or coal. This is confirmed by the CPI close to unity and by the low carbon number C_{max} in alkanes and alkenes, by the presence of PAH typical of vehicular gasoline and diesel emissions, and by the presence of aromatic hydrocarbons which may represent pyrolytic degradation products of coal. Although no molecular marker reported as typical of biogenic input has been detected, such as hydrocarbons around n-C_{29} (plant waxes) and/or fatty acids in the range n-C_{12}–C_{19} (microorganisms and plant waxes), it is interesting to note that in the iron-rich, gypsum free Aberdeen patinas (which, microscopically, are the ones displaying evidence for a limited amount of biological activity) we found a number of compounds (2-furaldehyde, the ketonic derivatives of cyclopentene and dibenzyl) which can be indirectly connected with biogenic sources. Of particular interest is the indirect evidence for the presence of polysaccharide gels which have been reported as common products of metabolic activities of bacteria, algae and fungi on rock substrates [9]. Py/GC-MS analysis of the thallus of two lichens from unpolluted locations (*Cetraria islandica* and *Cladonia arbuscula*) has indeed shown the presence of ketonic derivatives from the degradation of cellulose similar to the ones detected in Aberdeen's black patinas: 2-methyl-2-cyclopentenone, 2-methyl-cyclopentanone, 2-hydroxy-3-methyl-2-cyclopenten-1-one, 2,3-dimethyl-2-cyclopenten-1-one, 3,4-dimethyl-2-hydroxy-2-cyclopenten-1-one and 3-ethyl-2-hydroxy-2-cyclopenten-1-one. The presence of these pyrolytic degradation products of polysaccharides has also been reported in green biogenic layers underneath black sulphated crusts in the cathedral of Seville [22]. This preliminary chemical evidence (coupled with the SEM observations discussed above) suggests that biological activity may still play an important role in the build-up of thin dark patinas even in polluted urban areas [3,5].

5. Conclusions

Soiling processes in urban environments are responsible for the build-up of unsightly dark deposits (patinas) with a complex inorganic/organic chemical composition on the surfaces of granitic buildings. Two main types of dark patinas are reported here developing on granitic surfaces exposed to polluted urban atmospheres in Aberdeen and Dublin: (a) thick gypsum-rich crusts and (b) thin iron-rich patinas. The former are similar both in terms of composition and decay effects to the sulphate crusts already reported on other lithologies such as limestone and marble. As in those cases, their origin is due to the reaction between SO_2 pollution and Ca-bearing building material and is then directly connected with anthropogenic activities such as oil and coal combustion for domestic, vehicular and industrial needs. Anthropogenic airborne particles are included within the gypsum framework.

Gypsum crystallisation energies are responsible for severe physical disruption of the stone fabric leading to the detachment of granite fragments and incorporation of the same fragments within the growing crust. Through cracks and fractures, the gypsum crystallising front progrades inside the stone where there is also evidence for sulphate replacement (often pseudomorphic) of the original granite silicate mineralogy (in particular feldspars). The strong chemical and physical interaction between the sulphate patina and the granite suggests that a prompt removal of these crusts is needed to prevent further damage even though SO_2 levels in the Irish capital have now dropped considerably since the introduction of clean air regulations. Thin iron-rich patinas on granitic surfaces examined here are similar to soiling layers developing in polluted areas on low porosity building material such as quartz-cemented sandstones and brick [2]. Although containing evidence of a strong anthropogenic con-

tribution to their composition, these patinas also show features consistent with biological activity. Iron-rich soiling layers, although not showing the same degree of damage associated with sulphate-affected granite, are also interacting via dissolution episodes with the stone substrate and should be removed with a suitable cleaning technique which takes into account their complex composition.

Preliminary chemical analysis by Py-GC-MS of the patinas confirms, at least partly, the microscopic results. Both types of patina contain organic compounds (mainly aliphatic hydrocarbons and a few polycyclic hydrocarbons) typical of anthropogenic emission sources but in the iron-rich layers, there are also compounds that could represent the pyrolytic degradation products of biogenically derived material. Further analyses are being carried out to shed light on this important point.

Acknowledgements

This work has been carried out under the STEP project CT90-110 ('GRANITIX') of the EC. NS would like to thank Maureen Young (RGIT, Aberdeen), Tim Cooper and Paul O'Brien (Trinity College, Dublin) for their help in sorting out data collection and sampling. Ron Lee, Dudley Simons and Hilary Alberti provided technical assistance with the drafting and photographic material. Cambridge Earth Sciences Contribution no. 3787.

References

[1] T. Cooper, P. Dowding, J.O. Lewis, L. Mulvin, P. O'Brien, J. Olley and G. O'Daly, Contribution of calcium from limestone and mortar to the decay of granite walling, in N. Baer, C. Sabbioni and A. Sors (Eds.), Science, Technology and European Cultural Heritage, Butterworth-Heinemann, Oxford, 1991, pp. 456–461.

[2] A.G. Nord and T. Ericsson, Chemical analysis of thin black layers on building stone. Stud. Conserv., 38 (1993) 25–35.

[3] N. Schiavon, Microfabrics of weathered granite in urban monuments, in M.J. Thiel (Ed.), Conservation of Stone and Other Materials, Spon, London, 1993, pp. 271–278.

[4] B.J. Smith, R.W. Magee and W.B. Whalley, Weathering of granite in a polluted environment: Budapest, in A. Vicente-Hernandez, E. Molino Ballesteros, V. Rives-Arnau (Eds.), Alteration of Granites and Similar Rocks used as Building Materials, C.S.I.C. Madrid, 1993, pp. 159–162.

[5] N. Schiavon, G. Chiavari, D. Fabbri and G. Schiavon, Microscopical and chemical analysis of black patinas on granite, in V. Fassina (Ed.), Stone and Monuments: Methodologies for the Analyses of Weathering and Conservation. Proceedings of the IIIrd International Symposium on the Conservation of Monuments in the Mediterranean Basin, 1994, pp. 93–99.

[6] D. Camuffo, M. DelMonte, C. Sabbioni and O. Vittori, Wetting, deterioration and visual features of stone surfaces in an urban area. Atmos. Environ., 16 (1982) 2253–2259.

[7] B. Nagy, L.A. Nagy, M.J. Rigali, D.H. Krinsley and N.A. Sinclair, Rock varnish in the Sonoran Desert: microbiologically mediated accumulation of manganiferous sediments. Sedimentology, 38 (1991) 1153–1171.

[8] W.E. Krumbein and K. Jens, Biogenic rock varnishes of the Negev Desert (Israel): an ecological study of iron and manganese transformation by cyanobacteria and fungi. Oecologia, 50 (1981) 25–38.

[9] M. Robert and J. Berthelin, Role of biological and biochemical factors in soil mineral weathering, in, Interaction of Soil Minerals with Natural Organics and Microbes. Soil Sci. Soc. Am. Spec. Publ., 17, 453–495.

[10] P. Bennett and D.I. Siegel, Increased solubility of quartz in water due to complexing by organic compounds. Nature, 326 (1987) 684–686.

[11] R.C. Morris and A.B. Fletcher, Increased solubility of quartz following ferrous-ferric iron reactions. Nature, 330 (1987) 558–561.

[12] V. Verges-Belmin, Pseudomorphism of gypsum after calcite, a new textural feature accounting for the marble sulphation mechanism. Atmos. Environ., 28(2) (1994) 295–304.

[13] R.G. Maliva and R. Siever, Mechanism and controls of silicification of fossils in limestones. J. Geol., 96 (1988) 387–398.

[14] E.M. Winkler and P.C. Singer, Crystallisation pressures of salts in stone and concrete. Geol. Soc. Am. Bull., 83 (1972) 3509–3514.

[15] C. Saiz-Jimenez, Deposition of airborne organic pollutants on historic buildings. Atmos. Environ., 27B (1993) 77–85.

[16] B.R.T. Simoneit, Characterisation of organic constituents in aerosols in relation to their origin and transport: a review. Int. J. Environ. Anal. Chem., 23 (1986) 207–237.

[17] W.F. Rogge, M.A. Mazurek, L.M. Hildemann, G.R. Cass, and B.R.T. Simoneit, Quantification of urban organic aerosols at a molecular levels: identification, abundance and seasonal variation. Atmos. Environ., 27A (1993) 1309–1330.

[18] C. Saiz-Jimenez, Analytical approaches for the study of organic compounds in weathered building stones, in F. Veniale and U. Zezza (Eds.), Analytical Methodologies for the Investigation of Damaged Stones: Advanced Workshop, Pavia, 1990, 22 pp.

[19] W. Cautreels and K. van Cauwenberghe, Experiments on the distribution of organic pollutants between airborne particulate matter and the corresponding gas phase. Atmos. Environ., 12 (1978) 1133–1141.

[20] G. Chiavari and G.C. Galletti, Pyrolysis-gas chromatography/mass spectrometry of amino acids. J. Anal. Appl. Pyrolysis, 24 (1992) 123–137.

[21] C. Saiz-Jimenez, J. Grimalt, J. Garcia-Rowe and J.J. Ortega-Calvo, Analytical pyrolysis of lichen thalli. Symbiosis, 11 (1991) 313–326.

[22] C. Saiz-Jimenez, B. Hermosin, J.J. Ortega-Calvo and G. Gomez-Alarcon, Applications of analytical pyrolysis to the study of stony cultural properties. J. Anal. Appl. Pyrolysis, 20 (1991) 239–251.